CAMSAP1 breaks the homeostatic microtubule network to instruct neuronal polarity

Zhengrong Zhou[a,b], Honglin Xu[a], Yuejia Li[a,c], Mengge Yang[a,b], Rui Zhang[a], Aki Shiraishi[d], Hiroshi Kiyonari[d], Xin Liang[e,f], Xiahe Huang[a], Yingchun Wang[a,c], Qi Xie[g], Shuai Liu[h], Rongqing Chen[h], Lan Bao[i], Weixiang Guo[a,c], Yu Wang[a], and Wenxiang Meng[a,c,1]

[a]State Key Laboratory of Molecular Developmental Biology, Institute of Genetics and Developmental Biology, Innovation Academy for Seed Design, Chinese Academy of Sciences, 10019 Beijing, China; [b]College of Life Sciences, University of Chinese Academy of Sciences, 100049 Beijing, China; [c]College of Advanced Agricultural Sciences, University of Chinese Academy of Sciences, 100049 Beijing, China; [d]Laboratory for Animal Resources and Genetic Engineering, RIKEN Center for Biosystems Dynamics Research, 6500047 Kobe, Japan; [e]Tsinghua-Peking Joint Center for Life Science, School of Life Sciences, Tsinghua University, 100084 Beijing, China; [f]Max-Planck Partner Group, School of Life Sciences, Tsinghua University, 100084 Beijing, China; [g]Chinese Academy of Chinese Medical Sciences, 100700 Beijing, China; [h]Guangdong Province Key Laboratory of Psychiatric Disorders, Department of Neurobiology, School of Basic Medical Sciences, Southern Medical University, 510515 Guangzhou, China; and [i]State Key Laboratory of Cell Biology, Chinese Academy of Sciences Center for Excellence in Molecular Cell Biology, Institute of Biochemistry and Cell Biology, Chinese Academy of Sciences, 200031 Shanghai, China

Edited by Frank Bradke, German Center for Neurodegenerative Diseases, Bonn, Germany, and accepted by Editorial Board Member Yuh Nung Jan July 22, 2020 (received for review July 31, 2019)

The establishment of axon/dendrite polarity is fundamental for neurons to integrate into functional circuits, and this process is critically dependent on microtubules (MTs). In the early stages of the establishment process, MTs in axons change dramatically with the morphological building of neurons; however, how the MT network changes are triggered is unclear. Here we show that CAMSAP1 plays a decisive role in the neuronal axon identification process by regulating the number of MTs. Neurons lacking CAMSAP1 form a multiple axon phenotype in vitro, while the multipolar-bipolar transition and radial migration are blocked in vivo. We demonstrate that the polarity regulator MARK2 kinase phosphorylates CAMSAP1 and affects its ability to bind to MTs, which in turn changes the protection of MT minus-ends and also triggers asymmetric distribution of MTs. Our results indicate that the polarized MT network in neurons is a decisive factor in establishing axon/dendritic polarity and is initially triggered by polarized signals.

CAMSAP1 | MARK2 | noncentrosomal microtubules | neuronal polarity | cell migration

A typical mature neuron has one axon and multiple dendrites, providing the physical basis of neuronal function (1). In neurons, the establishment of axon/dendrite polarity is regulated by various factors, including the polarization of signaling regulators and the cytoskeletons (2–4). However, how the axon/dendrite polarity of neurons is established and how these determinants are precisely coordinated in the polarity establishment process remain poorly understood.

Microtubules (MTs) play a decisive role in axon/dendrite polarity differentiation in neurons, and various biophysical properties of MTs are known to be associated with this process (5). In the early axon/dendrite polarity differentiation process of in vitro cultured hippocampal neurons, accompanied by the first minor processes that rapidly grow and differentiate into axons, the number of MTs in the axon is significantly increased, and they are uniformly oriented to accommodate changes in neuronal morphology (6, 7). MT stability has also been shown to be associated with axon identification. MTs are more stable in the future axon than in a minor process, and this unbalanced distribution of stable and unstable MTs manifests from the second stage of axon/dendrite polarization differentiation (8). Also, changes in posttranslational modifications (PTMs), such as acetylated and detyrosinated modified MTs, have been shown to be related to this process (9). However, it is unclear which properties of MTs play essential decisive roles in axon/dendritic differentiation of neurons.

In neuronal cells, the MT network is composed mainly of noncentrosomal MTs (10). The calmodulin-regulated spectrin-associated proteins (CAMSAPs) bind to the minus-ends of noncentrosomal MTs and play an essential role in regulating the noncentrosomal MT network (11, 12). Studies have shown that Patronin, a CAMSAP homolog in *Drosophila*, can regulate the orientation of MTs in dendrites and is vital for dendritic pruning (13, 14). In mammalian cells, CAMSAP has three homologs that are associated with multiple neuronal functions and neurologic diseases. Studies have shown that CAMSAP2 and CAMSAP3 are associated with dendritic branches and axon differentiation, respectively (15, 16). These data suggest that in mammalian neurons, noncentrosomal MTs have multiple functions that are complex and finely regulated, but the molecular mechanism underlying these functions remains unclear.

In the present study, we focused on CAMSAP1 and found that it plays a decisive role in neuronal axon-dendrite differentiation as well as in the normal development and function of the cerebral cortex. Neurons lacking CAMSAP1 will form a multiple axon phenotype in vitro while the multipolar-bipolar transition and radial migration are blocked in vivo. We demonstrate that

Significance

Proper formation of axon/dendrites is critical for the neuron to fulfill its function, and microtubules are the final performer in this process. However, how polarizing signals transduce to microtubules to instruct axon/dendrite differentiation remains unknown. Here we found that CAMSAP1, a microtubule minus-end binding protein, drives neuronal polarization, migration, and cortical lamination. We also demonstrate that the microtubule-binding ability of CAMSAP1 is critical for the protection of microtubule minus-ends and preservation of the "seeds" for microtubule regeneration, and this ability is regulated by MARK2. Thus, our findings reveal that CAMSAP1 controls neuronal polarization via triggering an unbalanced distribution of microtubules among neuronal processes; CAMSAP family members regulate axon formation by changing the quantity and quality of microtubules.

Author contributions: Z.Z. and W.M. designed research; Z.Z., Y.L., M.Y., R.Z., X.L., X.H., and S.L. performed research; A.S., H.K., X.L., Yingchun Wang, R.C., and W.G. contributed new reagents/analytic tools; Z.Z., H.X., Y.L., M.Y., X.H., Yingchun Wang, Q.X., R.C., L.B., W.G., Yu Wang, and W.M. analyzed data; and Z.Z. and W.M. wrote the paper.

The authors declare no competing interest.

This article is a PNAS Direct Submission. F.B. is a guest editor invited by the Editorial Board.

[1]To whom correspondence may be addressed. Email: wxmeng@genetics.ac.cn.

This article contains supporting information online at https://www.pnas.org/lookup/suppl/doi:10.1073/pnas.1913177117/-/DCSupplemental.

First published August 24, 2020.

polarity regulatory factor MARK2 kinase phosphorylates the serine at amino acid 1485 of CAMSAP1 and thereby regulates the ability of CAMSAP1 to bind and protect MT minus-ends. In fact, in the early stage of neuronal polarization, it is the unbalanced stability of the noncentrosomal MTs minus-ends that cause the asymmetric distribution of MTs, which in turn promotes the differentiation of axon and dendrite.

Results

CAMSAPs Are Expressed in the Neocortex and Hippocampal Neurons. Since the CAMSAP family has three proteins, we comprehensively analyzed the expression profiles of CAMSAPs in the cortex, hippocampus, and neurons. The expression level of CAMSAP1 reached a peak during postnatal day (P) 7 to 28 or days in vitro (DIV) 4 to 7 (Fig. 1 *A–C*), indicating that CAMSAP1–3 have similar expression trends in brain development.

Then we generated a CAMSAP1 antibody suitable for immunostaining to investigate the distribution of CAMSAPs (*SI Appendix*, Figs. S1 *A–E* and S4 *C–E*). CAMSAP1 shows a high expression region change in the cortex during embryonic development, and it was concentrated in dendrites, but not in axons, at P0 (Fig. 1*D* and *SI Appendix*, Fig. S1 *F–H*). Moreover, CAMSAP2 was restricted to the cortical plate (CP) layer similar to CAMSAP1, but CAMSAP3 was strongly codistributed with callosal axons, which are enriched in the intermediate zone (IZ) and layer VI (Fig. 1*D*).

In cultured neurons, CAMSAP1 was detectable by immunostaining from stage 1 and distributed in neurites in stage 2. Even though CAMSAP1 had equal distribution in stage 2/3 neurons, it showed a preferential localization in dendrites and axonal growth cones in stage 3 neurons (Fig. 1 *E–H* and *SI Appendix*, Fig. S2 *A* and *B*). In contrast, CAMSAP2 and CAMSAP3 were preferentially located in the dendrites and proximal-middle region of axons, respectively (Fig. 1 *G* and *H* and *SI Appendix*, Fig. S2 *C* and *D*). All results indicate that CAMSAPs have different distribution patterns in the cortex and in cultured neurons.

***Camsap1* Knockout Mice Died of Epileptic Seizure.** Previous studies reported the functions of CAMSAP2 and CAMSAP3 in the nervous system, but there have been no such studies describing CAMSAP1. To investigate the function of CAMSAP1, we generated a line of *Camsap1* null allele mice by a gene knockout (KO) method. Animals carrying both null alleles are designated *Camsap1*($^{-/-}$) (*SI Appendix*, Fig. S3 *A–C*). The expression levels of CAMSAP2 and CAMSAP3 had no compensatory effect on

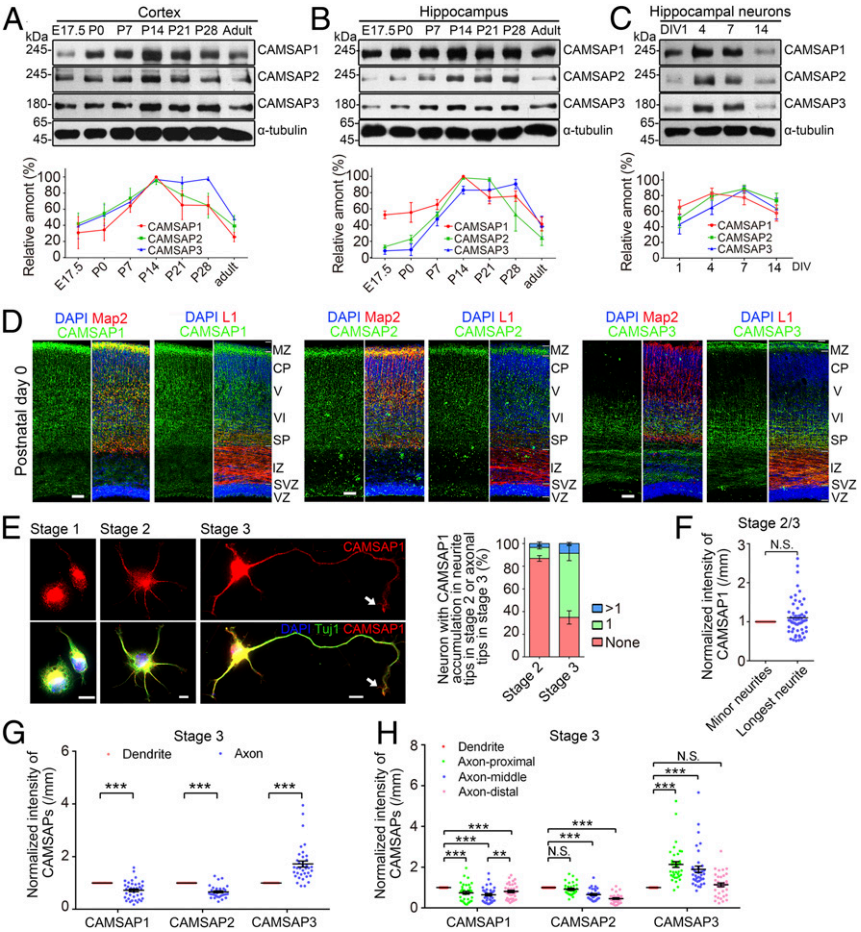

Fig. 1. CAMSAP1 expression in the developing cortex and cultured hippocampal neurons. (*A–C*, *Upper*) Western blot analysis of the expression levels of CAMSAPs in the cortex (*A*), hippocampus (*B*), and cultured neurons (*C*). (*A–C*, *Bottom*) Quantification analysis of the protein expression in *A–C* (n = 3 to 8 groups per condition). (*D*) Distribution of CAMSAPs in coronal sections of the cerebral cortex at P0. Map2 and L1 label the dendrites and callosal axons in mature neurons, respectively. (*E*, *Left*) distribution of CAMSAP1 in cultured neurons from stage 1 to stage 3. Arrows in stage 3 neuron indicate CAMSAP1 accumulation at the tip of the axon. (*E*, *Right*) Quantification analysis of neurons with CAMSAP1 accumulation in neurite tips of stage 2 or axonal tips of stage 3 (n = 161 and 183 neurons, respectively). (*F*) Quantification analysis of the distribution of CAMSAP1 in neurites from stage 2/3 (n = 57 neurons). (*G* and *H*) Quantification analysis of the total (*G*) and segmental (*H*) distribution of CAMSAPs in dendrites and axons from stage 3 neurons (n = 36 and 39 neurons, respectively). Data represent mean ± SEM. N.S., not significant ($P > 0.05$). ***$P < 0.001$, paired Student's t test. (Scale bars: 10 μm in *E*; 50 μm in *D*.)

CAMSAP1 deletion (*SI Appendix*, Fig. S3*D*). *Camsap1*($^{-/-}$) mice showed smaller brain and body size compared to wild-type (WT) *Camsap1*($^{+/+}$) mice, accompanied by developmental disorders (*SI Appendix*, Fig. S3 *E–H*). However, the mortality in the first 2 d after birth was 50% higher in *Camsap1*($^{-/-}$) mice compared with *Camsap1*($^{+/+}$) and *Camsap1*($^{+/-}$) mice (*SI Appendix*, Fig. S3*I*), and the majority of the remaining *Camsap1*($^{-/-}$) mice died of epileptic seizure after they were past weaning age (P18 to P21) (*SI Appendix*, Figs. S3*J* and S4 *A* and *B* and Movie S1), suggesting that CAMSAP1 is very important for the normal functions of the nervous system. In addition, the expression of CAMSAP1 was also confirmed by immunostaining (*SI Appendix*, Fig. S4 *C–E*).

CAMSAP1 Is Required for Neuronal Polarization. To examine the biological functions of CAMSAP1 in neurons, we prepared neurons from KO mice and cultured them in vitro. At DIV3, most of the *Camsap1*($^{+/+}$) neurons formed normal polar morphology with one axon and several dendrites (Fig. 2 *A* and *B*). However, more than one-half of the *Camsap1*($^{-/-}$) neurons showed multiple axons and other polarity defects (Fig. 2 *A–F*). Interestingly, the polarity defects of cultured *Camsap1*($^{-/-}$) neurons could be successively restored by ectopic expression of CAMSAP1 and CAMSAP3, but not of CAMSAP2 (Fig. 2 *G* and *H*). More importantly, knockdown of CAMSAP3 promoted these phenomena in *Camsap1*($^{-/-}$) neurons (*SI Appendix*, Fig. S5 *A* and *B*), indicating that CAMSAP1 and CAMSAP3 have functional redundancy in neuronal polarization.

To rule out the possibility that CAMSAP1 plays a role in the neuronal polarity maintenance phase, we depleted CAMSAP1 in WT neurons or expressed CAMSAP1 in *Camsap1*($^{-/-}$) neurons at DIV3 and then cultured for another 3 d. The phenotypes of WT neurons or *Camsap1*($^{-/-}$) neurons could not be changed (*SI Appendix*, Fig. S5 *C* and *D*), suggesting CAMSAP1 is required for the establishment but not the maintenance of neuronal polarity.

To examine polarization in vivo, embryos were subjected to in utero electroporation (IUE). In WT, a significant proportion of cells were distributed in the radial migration zone (RMZ; cells migrating in this region adopt bipolar morphology), while most cells in *Camsap1* ($^{-/-}$) brains accumulated in the multipolar migration zone (MMZ; cells migrating in this region adopt multipolar morphology (Fig. 2*I*) (17, 18).

To study the multipolar–bipolar (MP-BP) transition more accurately, we divided the neurons in the cortex into four typical morphologies (Fig. 2*J*). A higher proportion of cells in the *Camsap1*($^{-/-}$) brains showed multipolar morphology compared with WT brains (Fig. 2*K*). The same phenotypes were also observed in embryonic day (E) 17.5 embryos with electroporated shRNA at E14.5 (Fig. 2 *L* and *M*). In addition, the Golgi apparatus of the upper MMZ neurons was disoriented if CAMSAP1 was depleted (*SI Appendix*, Fig. S5 *E* and *F*). Collectively, these results indicate that CAMSAP1 regulates the MP-BP transition of cortical neurons.

CAMSAP1 Is Required for Migration of Cortical Neurons and Cortical Lamination. To investigate whether the absence of CAMSAP1 affects the migration of cortical neurons, *Camsap1*($^{+/+}$) and *Camsap1*($^{-/-}$) embryos were subjected to IUE, and 44.1 ± 1.1% WT neurons were found in the CP, while 42.2% ± 2.2% CAMSAP1-deficient neurons showed significant accumulation in the IZ (Fig. 3 *A* and *B*). We then used a BrdU birth dating assay to investigate neuronal migration. In *Camsap1*($^{-/-}$) mice, a significant proportion of BrdU^{+} neurons remained in the IZ (Fig. 3 *C* and *D*), demonstrating the existence of migration in cortical neurons of *Camsap1*($^{-/-}$) mice. In another study, we confirmed these defects in radial migration using shRNA to knock down the expression of CAMSAP1 (Fig. 3 *E* and *F*). Moreover, off-target effects were excluded by ectopic expression of an shRNA-resistant construct (CAMSAP1^{R}), as two concentrations among the four tests partially improved neuronal migration. This result also suggests that CAMSAP1 may regulate neuronal migration in a more complex manner other than via ubiquitous expression of this protein in neurons (Fig. 3 *E* and *F* and *SI Appendix*, Fig. S1 *A* and *C*). We excluded the possibility that the observed radial migration defects were due to proliferation, differentiation, apoptosis, or radial scaffolding abnormalities (*SI Appendix*, Fig. S6).

We next examined the laminar formation of the neocortex in *Camsap1*($^{-/-}$) mice and found that the nucleus intensity and Map2-labeled cells of cortical laminar fluctuated less in these mice compared with *Camsap1*($^{+/+}$) mice (*SI Appendix*, Fig. S7). To further confirm this notion, we stained for Tbr1 and Cux1 to label neurons in the deep layers (VI) and upper layers (II to IV) of P0 mice. These organized structures were disturbed in *Camsap1*($^{-/-}$) mice (Fig. 3 *G–J*). Similar cortical laminar disorganization was also observed in P21 young adults (Fig. 3 *K–N*). These observations indicate that CAMSAP1 plays a role in cortical laminar organization.

MARK2 Phosphorylates CAMSAP1 via Interaction. To investigate the regulatory mechanisms in more depth, we screened for molecule regulators using an immunoprecipitation assay (*SI Appendix*, Fig. S8 *A* and *B*). Mass spectrometry analysis identified one of the precipitated materials as MT affinity-regulating kinase 2 (MARK2) (*SI Appendix*, Fig. S8*C*), also known as partition-defective 1b (par-1b) (19). Previous studies have shown that MARK2 is involved in the establishment of polarity and the instability of the MT network of cells (20–22), suggesting that MARK2 is a promising candidate for participating with CAMSAP1 in the regulation of neuronal polarization and migration.

We first confirmed the physical interaction between all CAMSAPs and MARK2 using an immunoprecipitation assay (Fig. 4*A*). Then we constructed a series of CAMSAP1-truncated mutants and found that the region of amino acids 1,287 to 1,464 of CAMSAP1 was coprecipitated with MARK2 (*SI Appendix*, Fig. S8 *D* and *E*). Similarly, using several MARK2-truncated mutants, we found that CAMSAP1 interacted only with the MARK2 spacer domain (*SI Appendix*, Fig. S8 *F* and *G*). These results indicate that the MARK2 spacer domain interacts with the C-terminal fragment (amino acids 1,287 to 1,464) of CAMSAP1.

Considering that MARK2 is a kinase that phosphorylates its substrate, we suspected that CAMSAP1 is phosphorylated by MARK2. To test this hypothesis, we performed a phosphorylation-dependent band shift assay using phos-tag reagents. Exogenous CAMSAP1 showed a band shift in the presence of MARK2, demonstrating that CAMSAP1 is phosphorylated by MARK2 (Fig. 4*B*). In further experiments, we used a series of MARK2 mutants that lack the kinase domain (CT) or spacer domain and tail (ΔST) and demonstrated that this phosphorylation was dependent on the interaction of CAMSAP1 and MARK2 (Fig. 4*B* and *SI Appendix*, Fig. S8*F*).

To identify which site on CAMSAP1 is phosphorylated by MARK2, the band corresponding Flag-CAMSAP1 expressed in the presence of MARK2 was analyzed and its phosphorylated sites were observed by mass spectrometry (*SI Appendix*, Fig. S9 *B–D*). To confirm those phosphorylated sites, the corresponding serine (S) or threonine (T) was replaced by alanine (A) in CAMSAP1, making them inaccessible to phosphorylation. When CAMSAP1 was cotransfected with these mutants, only S1485A exhibited no band shift, suggesting that MARK2 phosphorylated the S1485 of CAMSAP1 (Fig. 4*C*). In supporting these results, it was also observed that MARK2 could not phosphorylate the truncated mutant lacking the CKK domain (CAMSAP1-ΔCKK; S1485 is located in the CKK domain) either in vivo or in vitro (Fig. 4 *D–F*). Interestingly, the identified serine residue is evolutionarily conserved in CAMSAP1 and CAMSAP3, but not in CAMSAP2 (Fig. 4*G*).

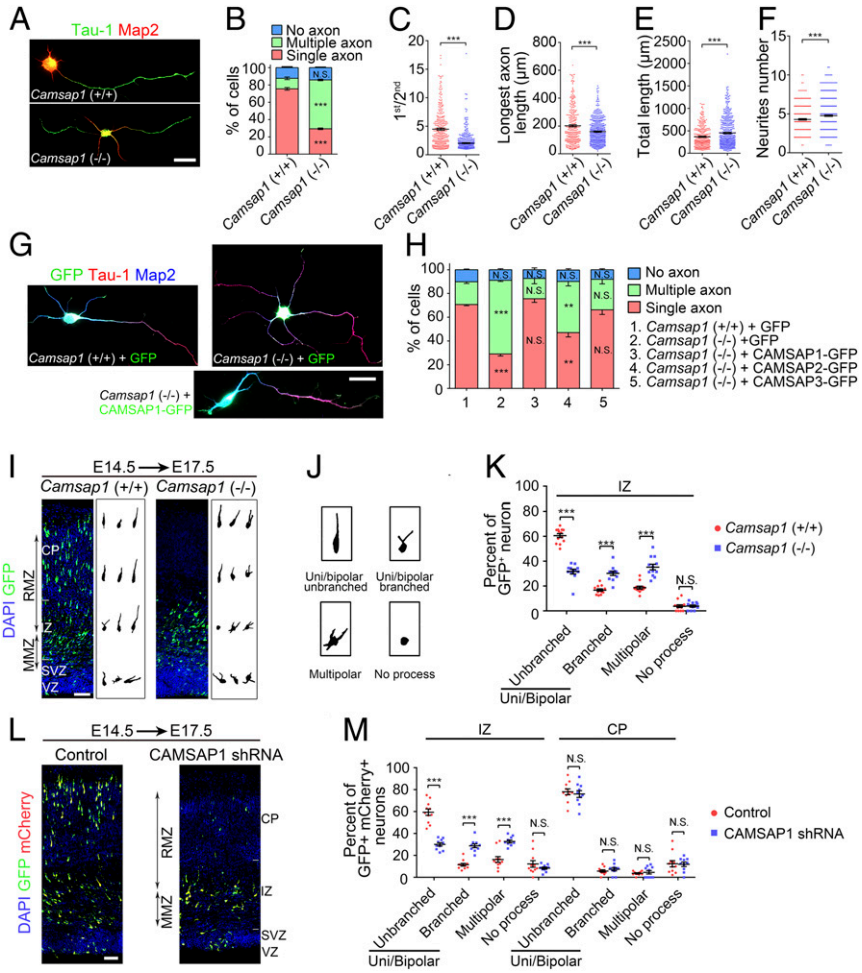

Fig. 2. CAMSAP1 regulates neuronal polarization. (*A*) Representative images of in vitro cultured neurons from *Camsap1*($^{+/+}$) and *Camsap1*($^{-/-}$) mice at DIV3. Tau-1 (axons), Map2 (dendrites). (*B*) Percentage of neurons with single, multiple, and no axons in *A*. (*C–F*) Ratio of the lengths of the longest and the second-longest neurite (*C*), length of the longest neurite (*D*), total length of neurites per neuron (*E*), and number of neurites per neuron (*F*) ($n = 337$ and 449 neurons, respectively). (*G*) Immunostaining for GFP, Tau-1, and Map2 in in vitro cultured neurons at DIV3 after transfection with different plasmids. (*H*) Percentage of neurons with single, multiple, and no axons in *G* (n = 117 to 317 neurons per condition). (*I*) In mice at E14.5, the neocortex was subjected to IUE with GFP-encoding plasmid. (*Left*) Representative image of immunofluorescence staining for DAPI and GFP in cortical coronal sections from E17.5 embryos. (*Right*, *Inset*) The various morphologies of neurons in the cortex. (*J*) The neuron morphologies in *I* were divided into four classes. (*K*) Quantification analysis of different morphologies of neurons in the IZ (n = 870 and 415 neurons from four and three brains, respectively). (*L*) In mice at E14.5, the neocortex was subjected to IUE with mCherry-encoding shRNA, and a GFP-encoding plasmid was cotransfected to depict the neurons. Immunofluorescence staining for DAPI, GFP, and mCherry in cortical coronal sections from E17.5 embryos is shown. (*M*) Quantification analysis of different morphologies of neurons in the IZ and CP (n = 1,757 and 1,535 neurons from three brains, respectively). Data represent mean ± SEM. N.S., not significant ($P > 0.05$). ***$P < 0.001$, paired Student's t test. (Scale bars: 20 μm in *A* and *G*; 50 μm in *I* and *L*.)

Phosphorylation of S1485 Is Required for CAMSAP1 to Regulate Axon/Dendrite Differentiation. To investigate the functions of phosphorylated CAMSAP1 in axon-dendrite polarity differentiation, we generated an antibody specific for CAMSAP1 phosphorylated on S1485 (*SI Appendix*, Fig. S9 *E–H*). We observed that total CAMSAP1 expression peaked earlier than its phosphorylation of S1485, which gradually increased from DIV2 and peaked at DIV7 (Fig. 5*A*), suggesting that phosphorylation of CAMSAP1 begins to function early in neuronal differentiation.

To determine whether phosphorylation at S1485 of CAMSAP1 is required for its function in regulating neuronal polarization, CAMSAP1 and its mutants were transfected into *Camsap1*($^{-/-}$) neurons. Even though S1485A exhibited limited function in rescue experiments, only S1485D (aspartic acid), which mimics MARK2-phosphorylated CAMSAP1, could rescue the phenotype of *Camsap1*($^{-/-}$) neurons like WT CAMSAP1 (Fig. 5 *B* and *C*). Further experiments clarified that this difference was caused directly by the replacement of S1485, since these two mutants have the same expression level (Fig. 5*D*). More importantly, the phenotype of multiple axons caused by MARK2 deletion can also be partially restored by S1485D, but not by WT CAMSAP1 (S1485 of WT CAMSAP1 cannot be phosphorylated under these conditions) (Fig. 5 *E* and *F*). Given that the phosphorylation of tau was unchanged in *Camsap1*($^{-/-}$) brains (*SI Appendix*, Fig. S10 *C* and *D*), we consider the result of partial rescue reasonable, as the phosphorylation of tau cannot be restored (19, 21). Taken together, these results suggest that CAMSAP1 works downstream of MARK2, and that phosphorylation rather than dephosphorylation of CAMSAP1 plays a critical role in neuronal polarization.

Phosphorylation of S1485 Reduces the MT-Binding Ability of CAMSAP1 and Affects MT Number. Since the CKK domain is required for the MT-binding ability of CAMSAP1, we hypothesized that phosphorylation of CAMSAP1 might alter its ability to

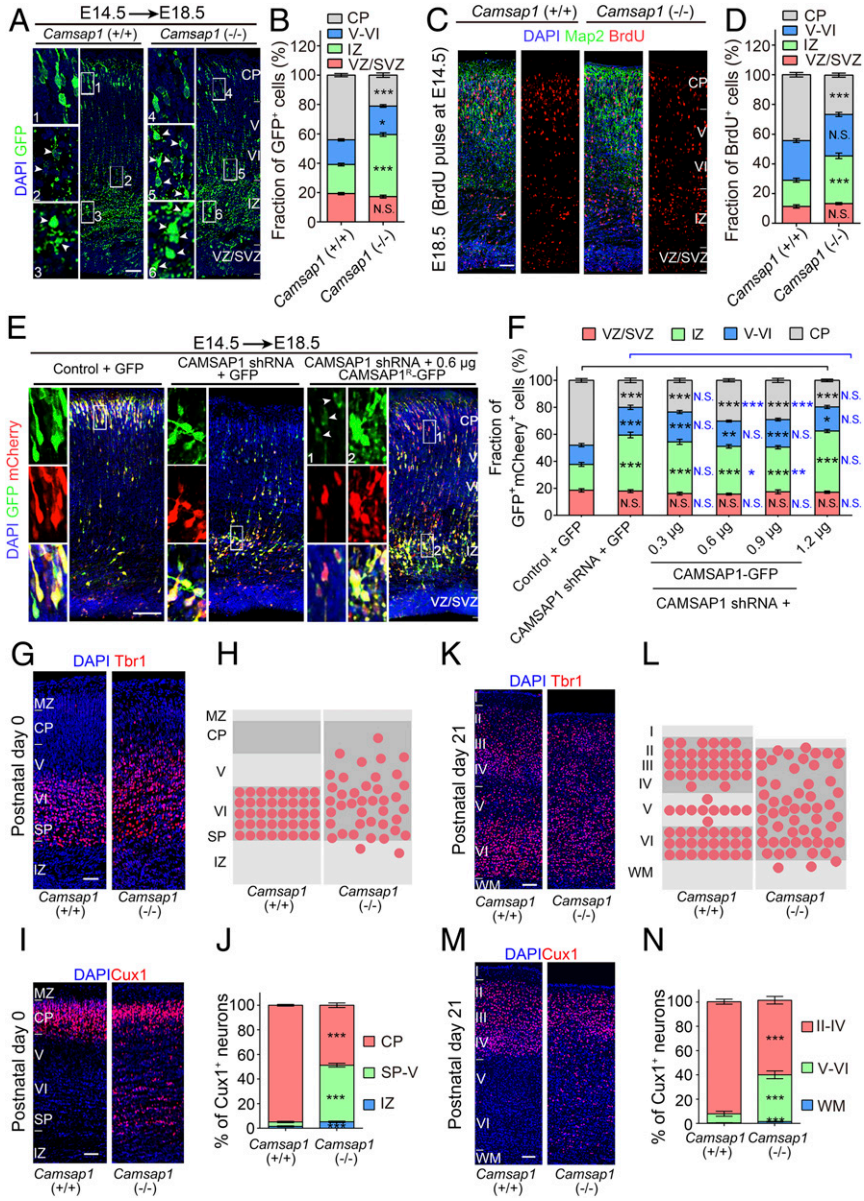

Fig. 3. CAMSAP1 regulates radial migration and cortical lamination. In mice at E14.5, the neocortex was subjected to IUE with GFP-encoding plasmid (*A*) or mCherry-encoding shRNA plus GFP- or CAMSAP1^{R}-GFP-encoding plasmid (E). (*A*) Immunostaining for DAPI and GFP in the cortical coronal section from E18.5 embryos. Arrowheads indicate the neurons. (*B*) Quantification analysis of the distribution of GFP^{+} neurons across different cortical regions (n = 5,293 and 3,838 neurons from four and five brains, respectively). (*C*) Pregnant mice were injected with BrdU at E14.5. Coronal sections of brain collected at E18.5 were analyzed by immunostaining for DAPI, Map2, and BrdU. (*D*) Quantification analysis of the distribution of BrdU^{+} neurons across the different cortical regions (n = 4,702 and 3,881 neurons from three brains, respectively). (*E*) Staining for DAPI, GFP, and mCherry in cortical coronal sections from E18.5 embryos. Arrowheads indicate the neurons that migrated to the CP. (*F*) Quantification analysis of the distribution of GFP^{+} and mCherry^{+} neurons across the different cortical regions in *E* (n = 3,683 to 4,538 neurons from four to five brains per condition). (*G* and *K*) Representative images of the distribution of Tbr1^{+} neurons. Immunofluorescence staining for DAPI and Tbr1 in the cortex from P0 mice (*G*) and P21 mice (*K*). (*H* and *L*) Schematic diagrams of the distribution of TBR1^{+} neurons in *G* and *K*. (*I* and *M*) Representative images of the distribution of Cux1^{+} neurons on immunofluorescence staining for DAPI and Cux1 in the cortex from P0 mice (*I*) and P21 mice (*M*). (*J* and *N*) Quantification analysis of the Cux1^{+} neurons in *I* and *M* (n = 2,327 to 13,686 neurons from four and three brains, respectively). Data represent mean ± SEM. N.S., not significant ($P > 0.05$). (*$P < 0.05$, **$P < 0.01$, ***$P < 0.001$, paired Student's t test. (Scale bars: 50 μm in *A*, *C*, *G*, and *I*; 100 μm in *E*, *K*, and *M*.)

bind to MT. We performed in vitro MT-binding experiments. GFP-tagged CAMSAP1 and its mutant proteins were purified and then incubated with Taxol-stabilized MT seeds (Fig. 6 *A* and *B*). Total internal reflection fluorescence (TIRF) microscopy images showed that WT CAMSAP1 accurately tracked MT minus-ends and poorly bound the MT lattice as previous reports have shown (23). Relative to WT, CAMSAP1 mutated from asparagine to alanine at position 1482 (N1482A) bound to a greater extent to MT minus-ends and lattice (Fig. 6 *B* and *C*), consistent with previous studies (24). Analysis of the CAMSAP1 S1485A mutant, which cannot be phosphorylated by MARK2, revealed a slight increase of its MT minus-end binding ability and a decrease in its distribution in the lattice. The CAMSAP1 S1485D mutant exhibited weaker binding to both MT minus-ends and lattice compared with WT. Finally, the ability of CAMSAP1 to bind MT minus-ends and lattice decreased to the

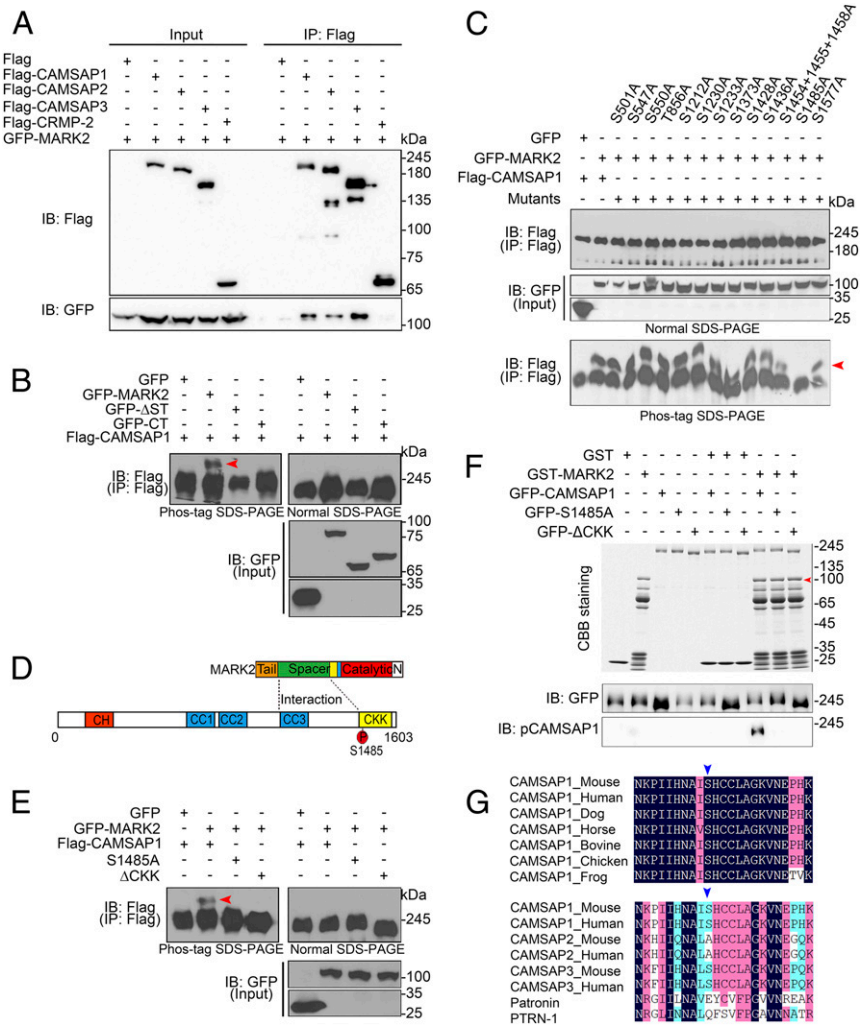

Fig. 4. MARK2 interacts with CAMSAP1 and phosphorylates S1485 of CAMSAP1. Phos-tag was used in SDS/PAGE, and the red arrowheads indicate the shifted bands caused by phosphorylation in *B*, *C*, and *E*. (*A*) MARK2 associates with CAMSAPs. HEK293 cells were cotransfected with the indicated plasmids, and then their lysates were subjected to immunoprecipitation with anti-Flag antibodies and proteins were detected by immunoblotting. Microtubule binding protein CRMP-2 served as a negative control. (*B*) MARK2 phosphorylates CAMSAP1 via the interaction between CAMSAP1 and MARK2. (*C*) MARK2 phosphorylates CAMSAP1 at S1485. A potential phosphor site was mutated into Ala to prevent the phosphorylation. (*D*) Schematic diagram showing the relationship between MARK2 and CAMSAP1. (*E*) The MARK2-dependent phosphorylation site of CAMSAP1 is located in the CKK domain. (*F*) Bacterially produced MARK2 was incubated with CAMSAP1 or its mutants to perform an in vitro kinase assay. The red arrowhead designates the band of GST-MARK2. (*G*) Sequence alignment of CAMSAP1 orthologs across species (*Upper*) and of CAMSAP/Patronin/PTRN-1 family members (*Lower*). Arrowheads indicate the S1485 of CAMSAP1.

greatest extent after removal of its CKK domain (Fig. 6 *B* and *C*).

To further study the regulatory mechanism of CAMSAP1 phosphorylation on the microtubule network, we conducted in vitro experiments using the foregoing proteins. First, an in vitro MT assembly assay revealed that CAMSAP1 was able to increase the amount of MTs in a concentration-dependent manner (Fig. 6*D*). Of note, equal amounts of CAMSAP1 or its mutants influenced MT assembly in proportion to their ability to bind to MTs (Fig. 6 *C* and *E*). Moreover, S1485D did not influence the length of MTs (Fig. 6 *G* and *H*). Taken together, these data indicate that the phosphorylation of CAMSAP1 functions in MT assembly by regulating its number rather than its length.

Like centrosome to centrosomal MTs, the minus-ends of noncentrosomal MTs not only are responsible for anchoring, but also function as "seeds" for MTs (25). We then asked whether CAMSAP1 could regulate the stability of these MT seeds by phosphorylation and thereby promote MT assembly. To test whether CAMSAP1 has a protective effect on MT seeds, we added nocodazole to depolymerize MTs in the same experiment (Fig. 6*F*). In this experiment, the plus- and minus-ends of the MTs have the same risk of depolymerization, while CAMSAP1 does not protect the plus-ends. Therefore, the total amount of MTs after treatment with nocodazole can reflect the stability of minus-ends of MTs—that is, the MT seeds. Our results showed that MT underwent brief depolymerization and then resumed growth. Nonetheless, these phenomena were more pronounced in the presence of WT and CAMSAP1 S1485A mutants, for example, at the time points of 30 and 40 min, respectively (Fig. 6*F*).

To directly measure the minus-end protection ability, tubulin dilution experiments were performed. We grew dynamic microtubule extensions from GMPCPP-stabilized microtubule seeds and while imaging, washed out the soluble tubulin to induce depolymerization in the absence or presence of CAMSAP1

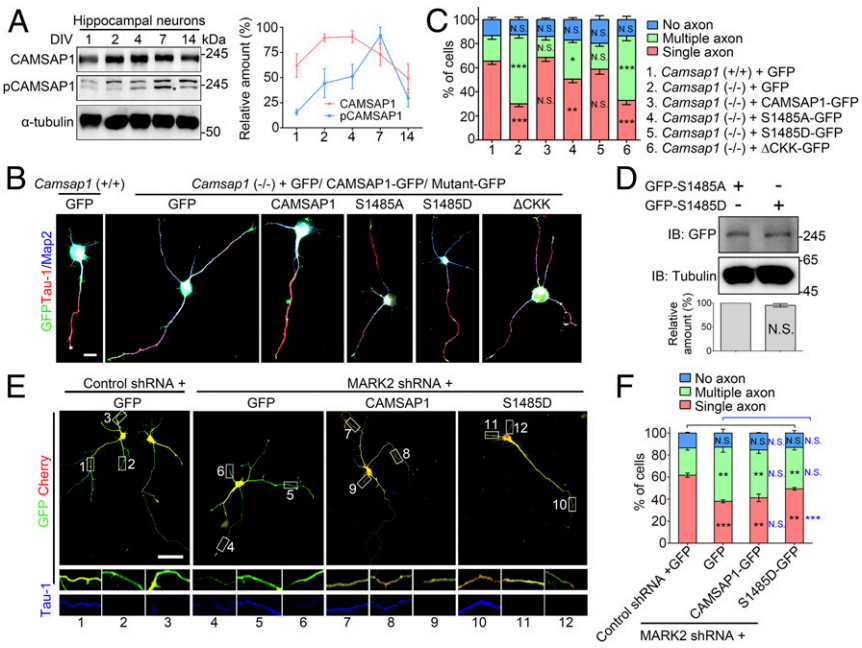

Fig. 5. CAMSAP1 controls neuronal polarity in response to the activity of MARK2. (*A*, *Left*) Western blot analysis of the protein levels of pCAMSAP1 (S1485) in cultured neurons. The asterisk shows the band of pCAMSAP1. (*A*, *Right*) quantification analysis of the protein expression on the left ($n = 5$). (*B*) Representative images of immunofluorescences staining for GFP, Tau-1, and Map2 in the neurons at DIV3 after transfection with indicated plasmids. (*C*) Quantification analysis of neurons with a single axon, multiple axons, or no axon in *B* ($n = 159$ to 366 neurons per condition). (*D*) Western blot analysis of the expression levels of S1485A and S1485D in neurons ($n = 3$). (*E*) Representative images of immunofluorescences staining for GFP and mCherry (*Upper* and *Middle*) and Tau-1 (*Bottom*) in the neurons at DIV3 after transfection with indicated plasmids. (*F*) Quantification analysis of *E* ($n = 220$ to 245 neurons per condition). Data represent mean ± SEM. N.S., not significant ($P > 0.05$). *$P < 0.05$, **$P < 0.01$, ***$P < 0.001$, unpaired Student's *t* test. (Scale bars: 50 μm.)

(Fig. 6*I*). We found that CAMSAP1 protected the MT minus-ends to resist depolymerization as shown previously (Fig. 6*J*) (23). In addition, the trend in variation of the depolymerization rate of CAMSAP1 and mutants corresponds with the amount of MTs (Fig. 6 *E*, *F*, and *J*), suggesting that stabilization of MT minus-ends is an important factor in MT network generation and regeneration.

Collectively, these results show that the phosphorylation of CAMSAP1 impairs its MT binding ability and reduces MT numbers.

Asymmetric Distribution of MTs Associated with CAMSAP1 Determines Polarization. The MT network goes through tremendous changes during neuronal polarization (6, 8). Interestingly, we and others have shown that CAMSAPs can bind with the minus-ends of noncentrosomal MTs to maintain the stability of MT seeds, thereby regulating the organization of the MT network (26, 27). Therefore, we speculated that CAMSAP1 might play the role of defender of MT seeds to control the MT network.

To test our hypothesis, we first examined the distribution of MT-associated CAMSAP1 clusters. The plasma membrane of neurons was permeabilized to remove soluble proteins before fixation, and the distribution of CAMSAP1 was observed by structured illumination microscopy (SIM). At stage 2/3, the MT-associated CAMSAP1 clusters showed accumulation in the longest neurite (Fig. 7 *A–C* and *SI Appendix*, Fig. S4*D*), indicating that the distribution of MT-associated CAMSAP1 was polarized during the neuronal polarizing process. Interestingly, the number of CAMSAP1 clusters per unit length of axon is lower than that of dendrite in stage 3 neurons (Fig. 7 *B* and *C*). These results, along with previous results, show that CAMSAP1 is unnecessary for maintaining neuronal polarity (*SI Appendix*, Fig. S5 *C* and *D*). Importantly, the distribution of CAMSAP1 clusters was positively correlated with the distribution of MTs (Fig. 7*D*). These findings, coupled with the results of our in vitro experiments, show that CAMSAP1 could protect the stability of MT seeds and then regulate the number of MTs (Fig. 6 *D–J*), indicating that the distribution of CAMSAP1 clusters might be closely linked to the tremendous changes in MTs occurring during neuronal polarization.

We next examined the characteristics of MTs in neuronal polarization. Consistent with previous reports, in stage 3, the difference in MT intensity was significantly increased in axons (Fig. 7 *E–G*). Finally, we examined *Camsap1*($^{+/+}$) neurons in stage 2-3, which began to show a polarized distribution of the MT network with a corresponding increase in MT signal intensity; however, no significant changes were observed in *Camsap1*($^{-/-}$) neurons (Fig. 7*H*). In addition, compared with *Camsap1*($^{+/+}$) neurons, the difference in MT intensity in each neurite also became significantly smaller (Fig. 7 *I* and *J*). Therefore, these data indicate that the asymmetric distribution of MTs associated with CAMSAP1 triggers an imbalance in the MT network to instruct neuronal polarity.

Previous studies have proven that the stability of MTs is sufficient to induce axon formation (8). To examine whether MT stability is also changed in *Camsap1*($^{-/-}$) neurons, microtubule retraction in the nocodazole treatment experiment and the phosphorylation state of Tau were measured; the results showed a similar change in *Camsap1*($^{-/-}$) and *Camsap1*($^{+/+}$) mice (*SI Appendix*, Fig. S10 *A–D*).

MT stability also has been shown to be associated with axon identification (8). Stable MTs are rich in detyrosinated tubulin (Glu-tubulin) and acetylated-tubulin (Ace-tubulin), while unstable MTs contain higher tyrosinated-tubulin (Tyr-tubulin) (9); therefore, we examined these three PTM of tubulins in P0 and P14 mice, as the expression of CAMSAP1 peaked at P14 (Fig. 1 *A–C*). Results from the cortex and hippocampus showed no significant change in *Camsap1*($^{-/-}$) mice (*SI Appendix*, Fig. S10*E*). Immunostaining using cultured neurons also showed

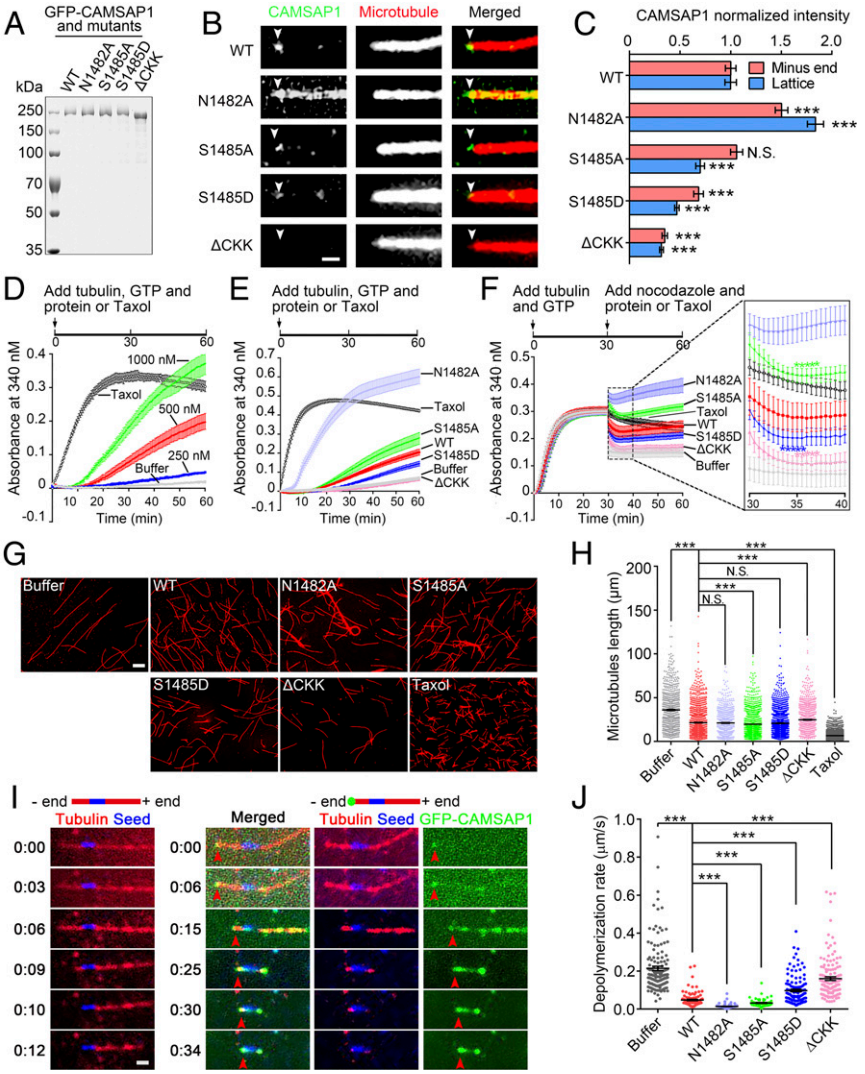

Fig. 6. Phosphorylation of CAMSAP1 alters its MT-binding ability. (*A*) CBB staining of a gel with GFP-CAMSAP1 and mutant proteins purified from sf9 cells. (*B*) Representative TIRF microscopy images of the MT-binding ability assay. Taxol-stabilized MTs were attached to the coverslip, and CAMSAP1 or mutant was added to the chamber to allow binding with MT minus-ends. (*C*) Quantification of CAMSAP1 and mutant intensities at MT minus-end and on the MT lattice (minus-end, $n = 38$ to 51 MTs per condition; lattice, $n = 52$ to 115 MTs per condition). (*D*) MT polymerization was monitored by measuring the absorbance (turbidity) at 340 nm for 60 min. Taxol (5 μM) or CAMSAP1 at different concentrations was mixed with the tubulin solution ($n = 3$). (*E*) MT polymerization was monitored by measuring absorbance at 340 nm for 60 min. Taxol (5 μM) or CAMSAP1/mutant (500 nM) was mixed with the tubulin solution ($n = 5$). (*F*) MT polymerization and depolymerization was monitored by measuring the absorbance (turbidity) at 340 nm. The tubulin solution was polymerized for 30 min, and then 5 μM Taxol or 400 nM CAMSAP1/mutant was mixed with 5 μM nocodazole and added to the solution to measure the absorbance for another 30 min ($n = 5$). The graph at right provides information on depolymerization, and statistical analyses were performed at the bottom of the curve between WT and mutants. (*G*) Representative images of MTs in *E* and tubulin labeled with cy3. (*H*) Length of MTs in *G* ($n = 684$ to 3,588 MTs per condition). (*I*) Representative time lapses of dilution experiments with buffer (*Left*) or GFP-CAMSAP1 (*Right*). Red arrowheads indicate the minus-end localization of CAMSAP1. The timestamp indicates the time after washout (min:s). (*J*) Quantification of MTs minus-end depolymerization rate in the presence of buffer, CAMSAP1, or mutants ($n = 60$ to 136 MTs per condition). Data represent mean ± SEM. N.S., not significant ($P > 0.05$). ***$P < 0.001$, unpaired Student's *t* test. (Scale bars: 1 μm for *B* and *I*; 10 μm for *G*.)

similar results (*SI Appendix*, Fig. S10*F*), suggesting that the absence of CAMSAP1 does not cause changes in PTM of MTs.

Since previous results have shown that Mec-17/αTAT1 plays a role in axon identification and branching (16, 28), we also used Mec-17 KO mice, *Mec-17*$^{(-/-)}$, to verify this possibility. Our results showed that in the absence of acetylated MTs, CAMSAP1-deficient neurons still exhibited multiple axon phenotypes (*SI Appendix*, Fig. S10 *G* and *H*), indicating that acetylation of MTs does not participate in the axon/dendrite differentiation of neurons mediated by CAMSAP1.

Collectively, these results strongly indicate that the phosphorylation of CAMSAP1 triggers an imbalance of MT networks to instruct neuronal polarity.

Discussion

In the early stages of neuronal polarity establishment, MTs are closely associated with neuronal morphological changes and play integral roles in neuronal axonal and dendritic differentiation (3, 5). However, the regulatory mechanism mediating MT function has remained elusive. In this investigation, we focused specifically on the regulatory devices that control the stability of

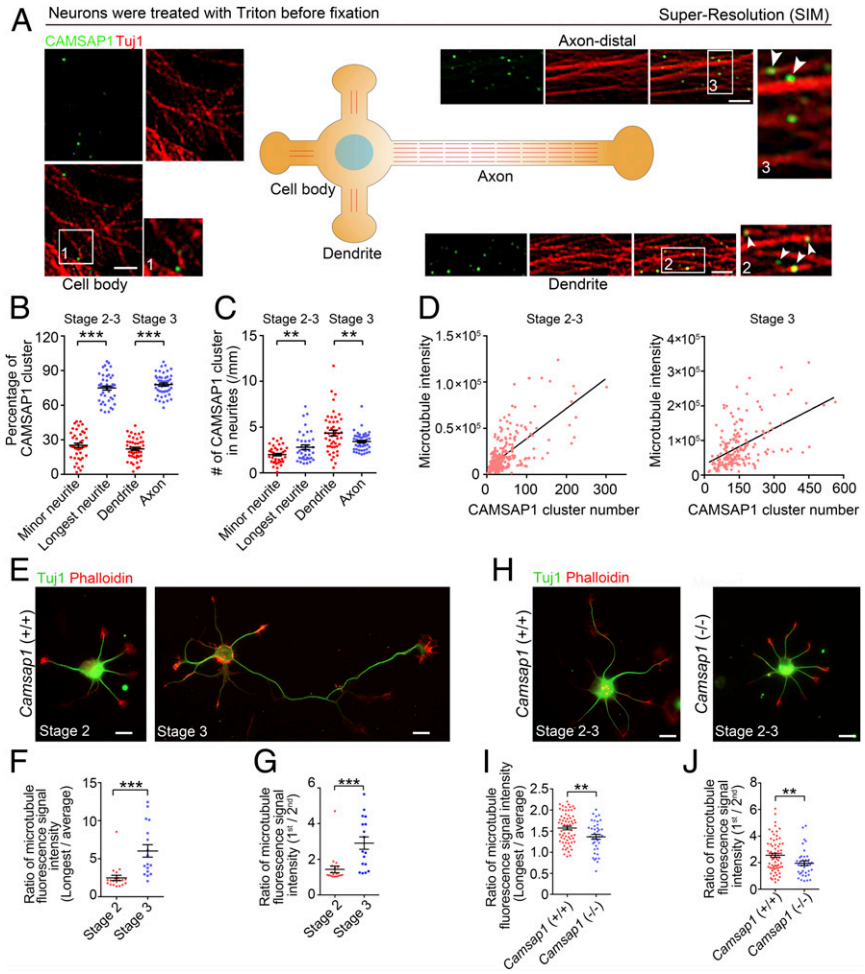

Fig. 7. CAMSAP1 is required for the asymmetric distribution of MTs. (*A*) Representative SIM images of CAMSAP1 in stage 3 cultured neurons after the removal of soluble substances. Panels 1, 2, and 3 show higher-magnification images, and the arrowheads in these panels indicate points at which CAMSAP1 interacts with MTs. (*B* and *C*) Quantification analysis of the percentage of MT-binding CAMSAP1 clusters in total (*B*) and per unit length (*C*) in minor neurites, the longest neurite of stage 2/3 neurons, and in the dendrite, the axon of stage 3 neurons (n = 44 and 47 neurons, respectively). (*D*) Fitted line plots of CAMSAP1 cluster number and microtubule intensity from neurons in *B* and *C*. (*E*) Representative images of immunostaining for Tuj1 and phalloidin in cultured WT neurons. (*F* and *G*) Ratio of fluorescence signal intensity in the longest neurite to the average signal intensity in all neurites (*F*) or of the longest neurite to the second-longest neurite (*G*) (n = 17 and 20 neurons, respectively). (*H*) Representative images of immunostaining for Tuj1 and phalloidin in cultured WT and *Camsap1*($^{-/-}$) neurons at stage 2–3. (*I* and *J*) Ratio of the fluorescence signal intensity in the longest neurite to the average signal intensity in all neurites (*I*) or of the longest neurite to the second-longest neurite (*J*) (n = 67 and 37 neurons, respectively). Data represent mean ± SEM. N.S., not significant ($P > 0.05$). ***$P < 0.001$; *$P < 0.05$, paired Student's t test. (Scale bars, 1 μm in *A*; 10 μm in *E* and *H*.)

noncentrosomal MT minus-ends, revealing the molecular mechanism of noncentrosomal MT minus-end protein CAMSAP1 as a target of the MARK2 signaling pathway, which triggers a change in the quantity of MTs and an unbalanced distribution of MTs between individual neuronal processes, and then controls axon identification (*SI Appendix*, Fig. S11). In addition, we have revealed the complex regulation of noncentrosomal MTs in mammals by uncovering the uniqueness of CAMSAP1 in the nervous system.

CAMSAPs in Neuronal Cells. CAMSAP family proteins, including Patronin in *Drosophila*, PTRN-1 in *Caenorhabditis elegans*, and CAMSAPs in mammals, have a C-terminal conserved globular domain (CKK domain) that binds to and stabilizes the minus-ends of MTs (12). We found CAMSAP expression in developing mouse brain and cultured neurons, corresponding to previous reports (15, 16). PTRN-1 and Patronin are both expressed in neuronal tissues (13, 29, 30) and, interestingly, are localized in both axon and dendrites (13, 30). In contrast, CAMSAPs have more complex distributions; CAMSAP2 is localized mainly to dendrites, while CAMSAP1 and CAMSAP3 are localized in the distal and proximal-middle regions of axons, respectively (Figs. 1 *E–H* and 7 *A–C* and *SI Appendix*, Fig. S2 *B–D*), suggesting that CAMSAPs have diverged and received more complex regulation in mammals to fulfill more sophisticated demands.

In *C. elegans*, the lack of PTRN-1 has been shown to impair neurite extension and branch retraction, but axonal outgrowth is developmentally normal (29, 31). Patronin could govern the orientation of MTs in dendrites to promote dendrite pruning in *Drosophila* (13, 14). In mammalian cells, CAMSAP2 is involved in dendrite development, while CAMSAP3 instructs neuronal polarity in a tubulin acetylation-dependent manner (15, 16). We have found that CAMSAP1 is required for axon/dendrite differentiation. Neurons lacking CAMSAP1 exhibited a multiple axon phenotype in vitro, and multipolar-bipolar transition and radial migration were blocked in vivo (Figs. 2 and 3). We did not observe the migration defect in the CAMSAP3 dc/dc mouse (16), however, although CAMSAP3 could rescue the multiple axon phenotype of *Camsap1*($^{-/-}$) neurons (Fig. 2*H*). Taken together, these results reflect a more precise regulation of the minus-ends of noncentrosomal MTs in higher mammals such as mice.

Phosphorylation of CAMSAP1 by MARK2 Kinase. Numerous signaling pathway regulators and the cytoskeleton are involved in the axon/dendrite differentiation process. MARK2/Par-1b is a Ser/Thr kinase that was identified initially as an MT affinity-regulating kinase. According to reports, MARK2 can control neuronal polarity and promote MT network instability (19, 21, 32, 33), but the relationship between them remains unknown. In our experiments, we have shown that MARK2 kinase directly phosphorylates CAMSAP1 S1485 to promote single axon growth (Fig. 5 *B* and *C*), reduce CAMSAP1 binding to MT minus-ends and lattice (Fig. 6 *B* and *C*), and affect the number of MTs (Fig. 6 *E* and *F*). In addition, the phosphor-mimicking CAMSAP1 mutant partially restored the phenotype of the MARK2 deletion causing multiple axons (Fig. 5 *E* and *F*), indicating that MARK2 regulates axon identification by influencing the interaction of CAMSAP1 with the minus-ends of noncentrosomal MTs.

Interestingly, the MARK2 phosphorylation site is well conserved in CAMSAP1 and CAMSAP3, but not in CAMSAP2 (Fig. 4*G* and *SI Appendix*, Fig. S9*A*), and the multiple axon phenotype in *Camsap1*$(^{-/-})$ neurons can be restored to WT levels by overexpression of CAMSAP1, the phosphor-mimicking CAMSAP1 mutant, or WT CAMSAP3, demonstrating that phosphorylation of CAMSAP1 has essential functions in the axon/dendrite differentiation process. Similar to CAMSAP2, the dephospho-mimicking CAMSAP1 S1485A shows only limited ability to rescue the polarity defects in *Camsap1*$(^{-/-})$, indicating that phosphorylation of CAMSAP1 plays a critical role in the axon decision process.

Phosphorylation of CAMSAP1 Controls the Asymmetric Distribution of MTs in Neurons. With the differentiation of axons/dendrites, the distribution of MT networks begins to become asymmetrical (7). It has been reported that MARK2 kinase works downstream of polarized signals, such as LKB1 and GSK3β, and that MARK2 could promote the instability of the MT network (2, 34). Our results indicate that MARK2 phosphorylation of CAMSAP1 could affect its binding affinity with MTs and reduce protection of the minus-ends of MTs (Fig. 6 *A*–*C*, *I*, and *J*). Supporting evidence was also provided by super-resolution microscopy showing that in polarizing neurons, although the distribution of total CAMSAP1 has not changed significantly (Fig. 1*F*), the distribution of CAMSAP1 clusters (MTs associated CAMSAP1) is asymmetric (Fig. 7*B*). Since stable minus-ends also function as seeds for MT network assembly (12), we propose that CAMSAP1 acts as a signal receiver, and that the corresponding polarity signal can affect the stability of the MT seeds by changing CAMSAP1 affinity to the minus-ends of MTs, regulating the number of MTs initiating asymmetric changes in the MT network and thus promoting axon/dendrite differentiation.

In addition, we did not find that the stability of MTs and their modifications to be involved in the regulation of CAMSAP1 (*SI Appendix*, Fig. S10 *A*–*F*). Unlike for CAMSAP3, removal of acetylation in MTs does not restore the phenotype of polarity defects caused by the deletion of CAMSAP1 (*SI Appendix*, Fig. S10 *G* and *H*). Our results regarding the regulation of MT stability do not contradict the previously reported regulation of neuronal polarity by CAMSAP3. CAMSAP3 is distributed mainly in axons and regulates the stability of MTs, while CAMSAP1 is distributed in both axons and dendrites and regulates asymmetric MT networks through its phosphorylation. More related research is needed to further refine the role of CAMSAPs in neuronal polarity.

In summary, we have revealed the role of the stability of the minus-ends of noncentrosomal MTs in the differentiation of axons/dendrites and the underlying molecular mechanisms. Our results also show that the absence of CAMSAP1 can cause dysplasia of the cerebral cortex and lead to epilepsy, suggesting that CAMSAP1 may be one of the pathogenic susceptibility genes of epilepsy, providing a basis for clinical research.

Materials and Methods

More detailed descriptions of the materials and methods used in this study are provided in *SI Appendix*, *Materials and Methods*.

Animals. All animal experiments were approved by the Animal Center of the Institute of Genetics and Developmental Biology (IGDB), Chinese Academy of Sciences, and by the Institutional Animal Care and Use Committee (IACUC) of RIKEN Kobe Branch, and were conducted in accordance with the IACUC guidelines at IGDB and RIKEN Kobe Branch. Mice were maintained in specific pathogen-free conditions in the animal facility and housed on a 12-h light/12-h dark cycle with ad libitum access to food and water.

Cell Culture, Transfection, and Immunofluorescence. Neurons were isolated from P0 mice and maintained in Neurobasal medium supplemented with 2% B27 (Gibco), 2 mM L-glutamine, and 1% penicillin/streptomycin (Gibco) at 37 °C in 5% CO_2. HEK293 cells were maintained in DMEM/F12 containing 10% fetal bovine serum and 1% penicillin/streptomycin at 37 °C in 5% CO_2.

Transfections were performing using Lipofectamine 2000 reagent or the Neon Transfection System (Invitrogen) according to the manufacturer's instructions.

For immunofluorescence, neurons and brain sections were blocked with goat serum and subsequently incubated with primary antibodies and secondary antibodies. Finally, the neurons and sections were mounted on slides with FluorSave reagent (MilliporeSigma).

Immunoprecipitation and Mass Spectrometry. The cultured cells or dissected tissues were lysed in cold buffer containing protease inhibitor mixture. After centrifugation to remove insoluble fraction and preclearing of the sample with protein G-Sepharose, antibody and protein G-Sepharose were incubated with the sample, followed by centrifugation to collect the protein.

For MS analysis, protein samples were loaded onto sodium dodecyl sulfate-polyacrylamide gel electrophoresis gels. The band was subjected to MS analysis after verification by Western blot analysis.

In Vitro MT Assays. Taxol-stabilized MT seeds were attached to the coverslips, and CAMSAP1-GFP or mutant was added to the flow chamber to measure the binding ability. Here 4 mg/mL tubulin was mixed with protein or drug in polymerization buffer on ice, and 1 mM GTP was added to the solution. The solution was transferred into a prewarmed 384-well plate, and tubulin turbidity was measured at 340 nm. For the MT depolymerization assay, nocodazole was transferred into the wells, and the tubulin turbidity was measured at 340 nm for another 30 min.

Statistical Analyses. Statistical tests were performed using GraphPad Prism, and a two-tailed Student's *t* test determined all statistical comparisons between the data. All of the data are represented as mean ± SEM.

Data Availability Statement. All pertinent data are available in the main text and *SI Appendix*.

ACKNOWLEDGMENTS. We thank Masatoshi Takeichi, Xu Zhang, Zhenge Luo, Zhiheng Xu, Yuqiang Jiang, Yongqing Zhang, and Shilai Bao for advice; Aihua Mao, Baoguo Li, Shuxin Wang, Peipei Xu, and Ninan Zhang for assistance with biochemical experiments and data analysis; Shuoguo Li for assistance with SIM; and Kangmin He and Jiachao Xu for help with TIRF microscopy. This work was supported by the National Natural Science Foundation of China (Grant 31871348) and the National Basic Research Program of China (Grant 2014CB942802).

1. S. J. Araújo, G. Tear, Axon guidance mechanisms and molecules: Lessons from invertebrates. *Nat. Rev. Neurosci.* **4**, 910–922 (2003).
2. M. Shelly, M. M. Poo, Role of LKB1-SAD/MARK pathway in neuronal polarization. *Dev. Neurobiol.* **71**, 508–527 (2011).
3. L. C. Kapitein, C. C. Hoogenraad, Building the neuronal microtubule cytoskeleton. *Neuron* **87**, 492–506 (2015).
4. P. W. Baas, A. N. Rao, A. J. Matamoros, L. Leo, Stability properties of neuronal microtubules. *Cytoskeleton (Hoboken)* **73**, 442–460 (2016).

5. C. Conde, A. Cáceres, Microtubule assembly, organization and dynamics in axons and dendrites. *Nat. Rev. Neurosci.* **10**, 319–332 (2009).
6. P. W. Baas, M. M. Black, G. A. Banker, Changes in microtubule polarity orientation during the development of hippocampal neurons in culture. *J. Cell Biol.* **109**, 3085–3094 (1989).
7. W. Yu, P. W. Baas, Changes in microtubule number and length during axon differentiation. *J. Neurosci.* **14**, 2818–2829 (1994).
8. H. Witte, D. Neukirchen, F. Bradke, Microtubule stabilization specifies initial neuronal polarization. *J. Cell Biol.* **180**, 619–632 (2008).
9. C. Janke, J. C. Bulinski, Post-translational regulation of the microtubule cytoskeleton: Mechanisms and functions. *Nat. Rev. Mol. Cell Biol.* **12**, 773–786 (2011).
10. F. Bartolini, G. G. Gundersen, Generation of noncentrosomal microtubule arrays. *J. Cell Sci.* **119**, 4155–4163 (2006).
11. W. Meng, Y. Mushika, T. Ichii, M. Takeichi, Anchorage of microtubule minus ends to adherens junctions regulates epithelial cell-cell contacts. *Cell* **135**, 948–959 (2008).
12. A. Akhmanova, C. C. Hoogenraad, Microtubule minus-end-targeting proteins. *Curr. Biol.* **25**, R162–R171 (2015).
13. C. Feng *et al*., Patronin-mediated minus end growth is required for dendritic microtubule polarity. *J. Cell Biol.* **218**, 2309–2328 (2019).
14. Y. Wang, M. Rui, Q. Tang, S. Bu, F. Yu, Patronin governs minus-end-out orientation of dendritic microtubules to promote dendrite pruning in Drosophila. *eLife* **8**, e39964 (2019).
15. K. W. Yau *et al*., Microtubule minus-end binding protein CAMSAP2 controls axon specification and dendrite development. *Neuron* **82**, 1058–1073 (2014).
16. V. Pongrakhananon *et al*., CAMSAP3 maintains neuronal polarity through regulation of microtubule stability. *Proc. Natl. Acad. Sci. U.S.A.* **115**, 9750–9755 (2018).
17. Y. Jossin, J. A. Cooper, Reelin, Rap1 and N-cadherin orient the migration of multipolar neurons in the developing neocortex. *Nat. Neurosci.* **14**, 697–703 (2011).
18. M. Barnat, J. Le Friec, C. Benstaali, S. Humbert, Huntingtin-mediated multipolar-bipolar transition of newborn cortical neurons is critical for their postnatal neuronal morphology. *Neuron* **93**, 99–114 (2017).
19. D. Matenia, E. M. Mandelkow, The tau of MARK: A polarized view of the cytoskeleton. *Trends Biochem. Sci.* **34**, 332–342 (2009).
20. A. Suzuki *et al*., aPKC acts upstream of PAR-1b in both the establishment and maintenance of mammalian epithelial polarity. *Curr. Biol.* **14**, 1425–1435 (2004).
21. Y. M. Chen *et al*., Microtubule affinity-regulating kinase 2 functions downstream of the PAR-3/PAR-6/atypical PKC complex in regulating hippocampal neuronal polarity. *Proc. Natl. Acad. Sci. U.S.A.* **103**, 8534–8539 (2006).
22. T. Sapir *et al*., Accurate balance of the polarity kinase MARK2/Par-1 is required for proper cortical neuronal migration. *J. Neurosci.* **28**, 5710–5720 (2008).
23. M. C. Hendershott, R. D. Vale, Regulation of microtubule minus-end dynamics by CAMSAPs and Patronin. *Proc. Natl. Acad. Sci. U.S.A.* **111**, 5860–5865 (2014).
24. J. Atherton *et al*., A structural model for microtubule minus-end recognition and protection by CAMSAP proteins. *Nat. Struct. Mol. Biol.* **24**, 931–943 (2017).
25. J. Roostalu, J. Rickman, C. Thomas, F. Nedelec, T. Surrey, Determinants of polar versus nematic organization in networks of dynamic microtubules and mitotic motors. *Cell* **175**, 796–808.e14 (2018).
26. N. Tanaka, W. Meng, S. Nagae, M. Takeichi, Nezha/CAMSAP3 and CAMSAP2 cooperate in epithelial-specific organization of noncentrosomal microtubules. *Proc. Natl. Acad. Sci. U.S.A.* **109**, 20029–20034 (2012).
27. A. Vemu *et al*., Severing enzymes amplify microtubule arrays through lattice GTP-tubulin incorporation. *Science* **361**, 1–12 (2018).
28. Dan Wei, α-Tubulin acetylation restricts axon overbranching by dampening microtubule plus-end dynamics in neurons. *Cereb. Cortex* **28**, 3332–3346 (2018).
29. J. D. Marcette, J. J. Chen, M. L. Nonet, The Caenorhabditis elegans microtubule minus-end binding homolog PTRN-1 stabilizes synapses and neurites. *eLife* **3**, e01637 (2014).
30. C. E. Richardson *et al*., PTRN-1, a microtubule minus end-binding CAMSAP homolog, promotes microtubule function in Caenorhabditis elegans neurons. *eLife* **3**, e01498 (2014).
31. M. Chuang *et al*., The microtubule minus-end-binding protein patronin/PTRN-1 is required for axon regeneration in C. elegans. *Cell Rep.* **9**, 874–883 (2014).
32. G. Drewes, A. Ebneth, U. Preuss, E. M. Mandelkow, E. Mandelkow, MARK, a novel family of protein kinases that phosphorylate microtubule-associated proteins and trigger microtubule disruption. *Cell* **89**, 297–308 (1997).
33. J. Biernat *et al*., Protein kinase MARK/PAR-1 is required for neurite outgrowth and establishment of neuronal polarity. *Mol. Biol. Cell* **13**, 4013–4028 (2002).
34. S. S. Deng *et al*., Protein kinase A rescues microtubule affinity-regulating kinase 2-induced microtubule instability and neurite disruption by phosphorylating serine 409. *J. Biol. Chem.* **290**, 3149–3160 (2015).